Gate-controlled Interaction Effects in 1D Quantum Channels

Yingshi Duo, Joshua Coop, Ian Farrer, David A. Ritchie, and Sanjeev Kumar, Senior Member, IEEE

Abstract— We present experimental results of electron transport in one-dimensional (1D) quantum channels created electrostatically with a triple-gate setup on GaAs/AlGaAs heterostructures. In this configuration, two gates determine the confinement potential, while the third gate adjusts the carrier density within the 1D channel. While maintaining a shallower confinement and decreasing the 1D carrier density, we observe interactions between the ground and first excited states, leading to an anticrossing. These states rely on the 1D carrier density, the decrease in confinement potential, and the effects of Coulomb interaction. Our results suggest that fine-tuning the triple-gate geometry may reveal complex phases in interacting 1D quantum systems.

I. INTRODUCTION

The transport properties of low-dimensional semiconductor nanostructures in high-quality GaAs/AlGaAs heterostructures have been extensively studied, especially using the twodimensional electron gas (2DEG). The ability to further confine electrons' momentum in the 2DEG by electrostatic potentials allows access to the 1D regime [1,2], where conductance measured at low temperatures quantizes in universal units of $2Ne^2/h$, where the factor 2 accounts for the spin degeneracy of electrons, h is Planck's constant, e is the electron charge, and N is the integer filling of 1D subbands [3-11]. Advances in fabrication techniques and access to highquality 2DEGs now make the many-body states within 1D channels accessible [5,9,12]. Several interesting features have been observed in the conductance of 1D quantum wires or quantum point contacts (QPCs), such as the $0.7(2e^2/h)$ conductance anomaly and the spin-polarized $0.5(2e^2/h)$ conductance feature [13-24]. Both are suggested to result from intrinsic spin polarization and exchange interactions within 1D channels, while the role of lateral spin-orbit effects has also been proposed [7,13,20,25]. Additionally, some reports indicate that these features may originate from localized impurities, similar to the Kondo effect [13]. Furthermore, the 0.7 anomaly has also been proposed to arise from the formation of a Wigner crystal within a 1D channel [26,27].

Research supported by the United Kingdom Research and Innovation (UKRI), Future Leaders Fellowship (MR/S015728/1; MR/X006077/1).

The Wigner crystal—a solid phase of electrons—was theoretically predicted by Eugene Wigner in 1934. Its formation relies on the dominance of electron-electron Coulomb repulsion over kinetic energy, which occurs at very low temperatures and densities [28]. Due to the enhanced interaction effects in 1D systems, the emergence of a 1D Wigner crystal remains a topic of fundamental interest [29]. This state forms when a confined system of 1D electrons interacting via the long-range Coulomb force minimizes its total energy by arranging into a regular lattice due to mutual repulsion. The key condition for this crystallization is that the Coulomb energy must surpass the kinetic energy in the lowdensity regime. However, intrinsic quantum fluctuations and inhomogeneity in the background potential within 1D channels could affect the direct observation of the 1D Wigner lattice. Moreover, challenges arise in manipulating a 1D Wigner lattice due to the lack of long-range order in infinite systems [27,28,30,31]. Nonetheless, it may be possible to probe phases of the 1D Wigner lattice, at least macroscopically in systems with few electrons. Experimental evidence of the 1D Wigner lattice was reported through conductance measurements in weakly confined 1D quantum wires, where the first plateau at $2e^2/h$ disappeared when the confinement and carrier density were reduced, indicating the new ground state at $4e^2/h$ [4,5,32]. Due to the increased interactions among 1D electrons, the ground state can transition into a zigzag phase before splitting into two lines of electrons, each contributing 2e²/h to conductance. This phenomenon was directly captured through transverse electron focusing experiments [33]. Moreover, minimizing disorder is essential to prevent pinning the fragile Wigner state. Additionally, lowdensity 1D systems revealed the emergence of a variety of quantized conductance plateaus below $2e^2/h$ at fractional fillings of 2/5,1/5, and others (in units of e^2/h) in the 1D Wigner regime [5.8,9].

Despite advances in understanding the physics of the 1D Wigner lattice, experimental challenges limit the extent of its observations due to the subtle balance required between carrier density and confinement potential. In the present work, we fabricate high-quality 1D quantum wires using GaAs/AlGaAs heterostructures and investigate the emergence of the 1D Wigner lattice through transport measurements.

II. EXPERIMENTAL

Two samples, A and B, were fabricated using the 2DEG formed within a GaAs/AlGaAs quantum well of 30 nm width, grown using molecular beam epitaxy. Samples A and B had a low-temperature mobility, μ of 2.38×10^6 cm²/Vs and carrier

Y. Duo, J. Coop, and S. Kumar are with the Department of Electronic and Electrical Engineering, University College London, Torrington Place, London WC1E 7JE, UK (phone: +44-20-7679-7758; e-mail: sanjeev.kumar@ucl.ac.uk).

I. Farrer is with the School of Electrical & Electronic Engineering, University of Sheffield, Mappin Street, Sheffield S1 3JD, UK.

D. A. Ritchie is with the Cavendish Laboratory, University of Cambridge, J. J. Thomson Avenue, Cambridge CB3 0HE, UK.

density, n_{2D} of 2.24×10^{11} cm⁻². The GaAs/AlGaAs wafers were converted into Hall bar geometries using the standard photolithography process. Ohmic contacts were formed on the edges of the Hall bar; the process is described in detail below. Metal gates (Cr/Au) were deposited on Hall bars to define triple-gated 1D devices consisting of a top gate separated from a pair of split gates by a cross-linked poly (methyl methacrylate), PMMA (Fig. 1(a)) [4,5,9]. The lithographically defined 1D channel had a length L of 0.7 μ m and a width W of 1 μ m. The two-terminal differential conductance, $G=dI/dV_{sd}$, where V_{sd} is the applied de sourcedrain bias, was measured in a cryogen-free dilution refrigerator at a base temperature of 19 mK. An excitation voltage of 10 μ V at 77 Hz was applied, and G was measured using the standard lock-in amplifier.

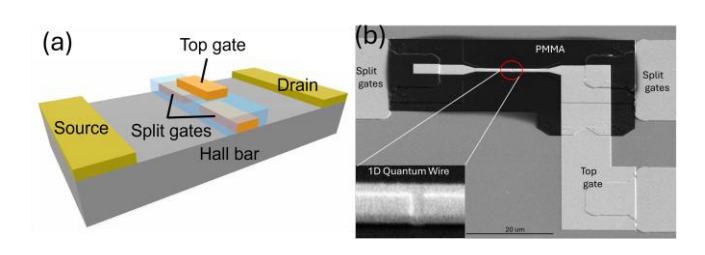


Figure 1: (a) Schematic of the device showing split gates, top gate, source, and drain for two-terminal conductance measurement. (b) Scanning electron microscopy image of a representative device, showing a pair of split gates with a top gate placed over them via PMMA, as indicated in the black regime. A magnified view of the central region of the 1D channel is shown at the bottom, where split gates and a top gate may be noticed.

III. DEVICE FABRICATION

In this work, ohmic contacts were formed on the edges of the Hall bar by diffusing an alloy of NiGeAu as spikes from the surface to create electrical connections with the 2DEG. To fabricate ohmic contacts, three processes are generally required: photolithography, thermal deposition, and rapid thermal annealing (RTA). The pattern of ohmic contacts on the photoresist was written using standard photolithography. After development, a NiGeAu alloy was thermally deposited on the surface, as shown schematically in Fig. 1(a), followed by lift-off. Au is known as a good metal conductor with low electrical resistivity. Ge acts as a donor that would substitute Ga in GaAs, providing extra electrons to improve conductivity [34-36]. Ni serves as a surfactant, which prevents spheroidization in the AuGe alloy and helps facilitate the diffusion of elements into GaAs. Additionally, the ratio of Au to Ge was set at 88 wt%: 12 wt% to limit the eutectic temperature at 360 °C [36]. After deposition, RTA treatment induces metal-semiconductor reactions, resulting in the diffusion and penetration of the alloy through the heterostructure and the 2DEG. As the annealing process begins and the temperature rises. Ni reacts with native oxides on the GaAs surface to eliminate their effects and interacts with GaAs, forming intermediate complexes. These complexes disrupt the crystal order, creating pathways for diffusion. Through these pathways, Ge diffuses into GaAs, while Ga diffuses out of GaAs, reacting with Au in the

contacts [35,36]. As described above, the components in the contacts react with GaAs to form thermodynamically stable compounds until the reactions are complete or reactants are exhausted [34-36]. Further annealing may cause As to diffuse from GaAs toward the contact surface, vaporize, and form voids that are later filled with other compounds. It has been reported that Ge doping in GaAs decreases contact resistance, whereas Ga diffusion increases it [37].

Fig. 2 shows the effects of RTA temperature and holding time on the resistivity of the 2DEG measured at a temperature

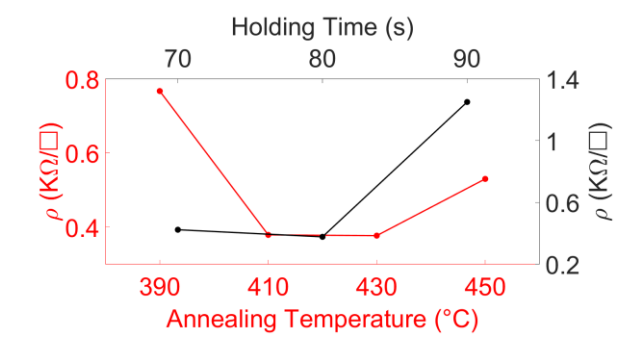


Figure 2: Resistivity measured between ohmic contacts as a function of annealing temperature (shown in red) and the holding time of RTA (shown in black).

of 77 K. We observed that as the annealing temperature increased from 390 to 450°C, the resistivity dropped sharply at 410°C, reached its lowest point at 430°C, and then increased again at 450°C. Additionally, the holding time was optimized at a fixed RTA temperature of 430°C, as shown in Fig. 2. It was concluded through multiple optimization tests that holding times between 70-80 s yielded consistently lower resistivity values. Similar results have also been found in other reports [37,38]. The decrease in resistivity as the temperature decreases could be explained by the increase in the diffusion of Au along the spikes, which leads to the increase in the Au-Ga mixture and heavy doping of Ge in the Ga vacancies in GaAs. Exceeding the lowest point in resistivity, higher annealing temperature keeps driving the reaction between Ga and Au, but the formation of Au-Ga mixture dominates the process, leading to the degradation in surface morphology of contacts and the increase in contact resistivity. Also, the instability of the bonds among the atoms in the heterostructure and contacts deteriorates the contact resistivity. Therefore, the effect of annealing temperature is determined by the Ge doping in the semiconductor, the surface degradation, and the stability of the bonds at high annealing temperatures [38]. For the effect of holding time, the resistivity reduced as the time increased from 70 to 80 s, and increased significantly as the time reached 90 s. The decrease in resistivity as the holding time increased may be attributed to further doping of Ge during a longer period, when the effect of Ge doping is dominant [36]. When the holding time is longer than the lowest resistivity point, the doping slows down due to the consumption of Ge, and the increase in Ga vacancies may in turn increase the contact resistivity [34].

The Schottky gates are used to selectively deplete electrons in the 2DEG to define a clean 1D channel. Au is ideal for the formation of a Schottky gate on GaAs due to its high electrical conductivity and availability as a bonding pad. However, due to its poor adhesion to GaAs, a thin Cr or Ti layer is generally sandwiched between Au and GaAs [36].

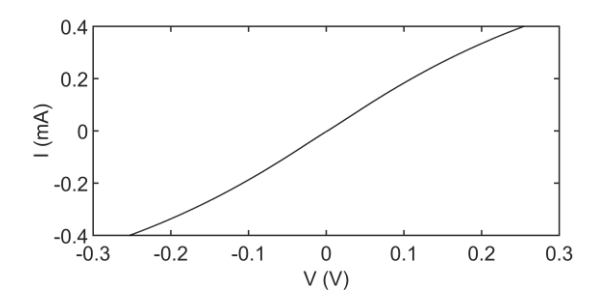


Figure 3: I-V curve of the fabricated ohmic contacts.

Fig. 3 shows the current-voltage (I-V) characteristics between two ohmic contacts, exhibiting linear ohmic behavior up to approximately \pm 200 mV. As the magnitude of applied voltage increases, the I-V curve tends to become nonlinear in both negative and positive bias, likely due to high local electric fields around the spikes formed within the heterostructure [39]. The high fields drive the electrons in the 2DEG to the maximum velocity. Therefore, further increase in the driving voltage does not increase the mobility of electrons, and the corresponding I-V curve deviates from the linear trend [39]. Conductance measurements were performed at an excitation voltage of 10 μ V, which is well within the linear regime. For larger dc bias voltage, the non-linear transport will occur, which is generally utilized to perform 1D subband spectroscopy [11].

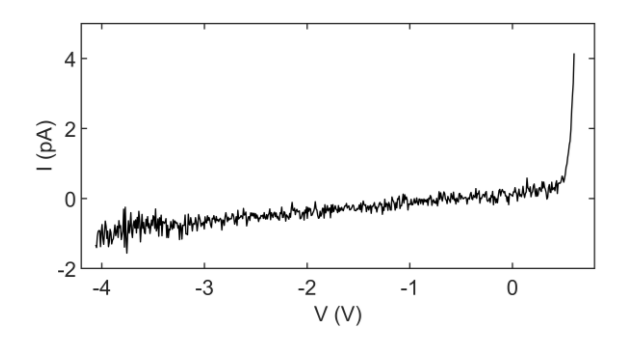


Figure 4: I-V curve representing the leakage-current measurement performed on Shottky gates.

The Schottky gates are characterized by measuring I-V characteristics between one of the gates (either the split gates or the top gate) and an ohmic contact. Fig. 4 shows the I-V curve of a Schottky gate, with a positive breakdown voltage of ~ 0.5 V and a leakage current of around 1 pA at V= -4.0 V. This low leakage current at high negative bias shows good Schottky diode characteristics in our devices.

IV. RESULTS AND DISCUSSION

The differential conductance G measured through a 1D constriction requires ramping (sweeping) the split gate voltage, V_{sg} to first deplete electrons underneath the gates, before the depletion zone extends in the region between the split gates to pinch off the channel. As the split gates begin to sweep from zero to negative voltage values, the 2D density of states (DoS) transforms into the 1D DoS, resulting in the onset of quasi-one dimensionality. The 1D channel forms, and

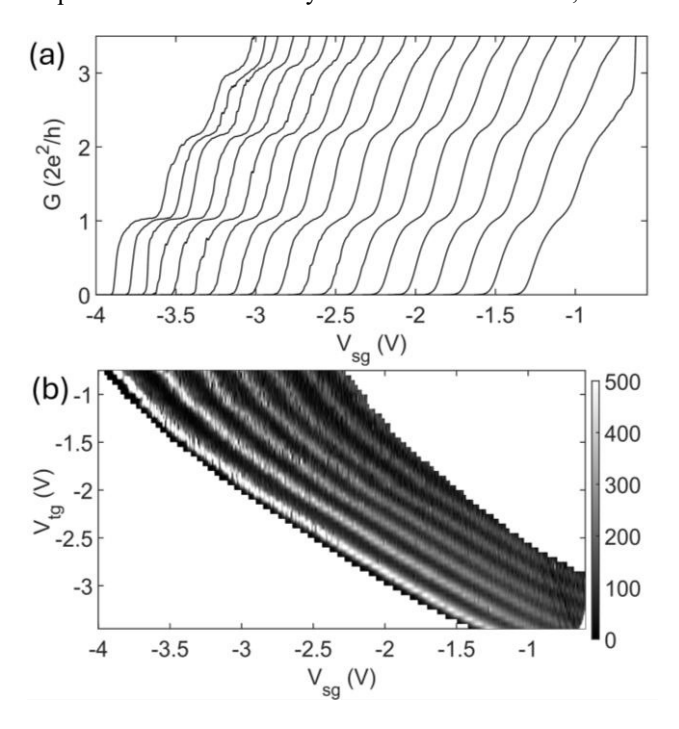


Figure 5: (a) The differential conductance G of Sample A at $V_{\rm g}$ from -0.75 V (left) to -3.45 V (right) with an increment of -0.15 V. (b) The corresponding grayscale plot of transconductance $dG/dV_{\rm sg}$ of data in Fig. 5(a).

depending on the dimensions of the 1D constriction and the Fermi energy, N integer 1D subbands will be occupied. By sweeping the split gates further negatively, electrons in higher subbands depopulate, resulting in the observation of a conductance staircase quantized in units(a) of $2e^2/h$ (Fig. 5(a)). Therefore, sweeping V_{sg} controls the width and the number of 1D subbands within the 1D channel. Applying a negative voltage to the top gate, V_{tg} reduces the electron density within the 1D channel, as well as affecting the overall confinement. The differential conductance was measured under different top gate and split gate voltages. The series resistance from measurement leads and ohmic contacts was removed from the results to align the quantized conductance plateaus with $N(2e^2/h)$.

Fig. 5(a) shows the differential conductance G of Sample A as a function of split gate voltage at different top gate voltages. One advantage of the top gate is that it assists in flattening the bottom of the potential confinement as the top gate voltage decreases, which also reduces the number of occupied 1D subbands. Also, as the split gate voltage controls

the width of the 1D channel, the decreasing top gate voltage raises the bottom of the potential confinement, thereby assisting in manipulating the Fermi level across the 1D energy states. In Fig. 5(a), on the left, integer plateaus in units of $2e^2/h$ are resolved. This is a strong confinement regime; the potential is generally parabolic. As the top gate voltage decreases from the left ($V_{tg}\sim$ -0.75 V) to the right ($V_{tg}\sim$ -3.45 V), the integer plateaus gradually weaken, and the overall channel width is reduced. It may be noted on the left of the

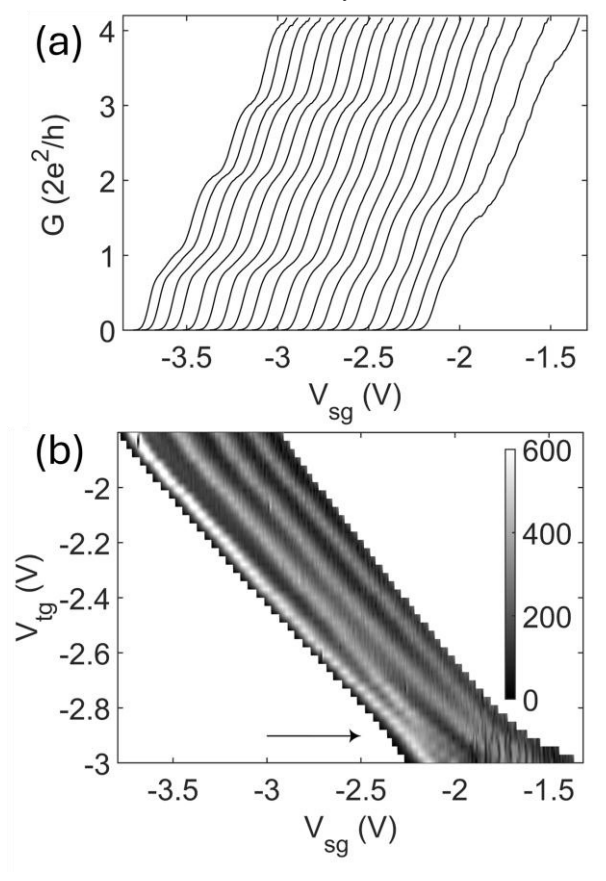


Figure 6: (a) The differential conductance G of Sample B at $V_{\rm g}$ from -1.80 V (left) to -3.0 V (right) with an increment of -0.06 V. (b) The corresponding grayscale plot of transconductance $dG/dV_{\rm sg}$ of data in Fig. 6(a).

plot that three subbands are occupied, whereas the trace on the right shows two plateaus significantly reduced in strength. On weakening the confinement, the subband spacing reduces, which means the system is transitioning towards two-dimensionality. The evolution of 1D subbands may be further visualized in the grayscale plot in Fig. 5(b), which shows the transconductance of the results presented in Fig. 5(a). The dark regime appears as plateaus, and the gray regime as the risers in conductance. It can be seen from the grayscale plot that five 1D subbands are resolved at $V_{tg} \sim$ -0.75 V, which gradually narrow in the plateau width as the density and confinement within the 1D channel decrease. Although the system displays well-defined plateaus and a consistent decrease in strength as the confinement is reduced, we did not observe signs of anticrossing between the ground and first

excited states, which is a precursor to the formation of the 1D Wigner lattice within the 1D channel.

Fig. 6 shows the conductance plot in Sample B as a function of split gate voltage for different top gate voltages. On the left of the graph, the $2e^2/h$ plateau, representing the ground state, is already weakly defined, although it is accompanied by the 0.7 structure. On decreasing the top gate voltage, the $2e^2/h$ plateau gradually disappears; notice the traces close to the pinch off regime near V_{sg} ~-2.5 V, which is accompanied by a relatively stronger plateau at $4e^2/h$. On moving further to the right, the $2e^2/h$ returns. It may be noticed that plateaus on the right of the plot are slightly lower in value than the expected quantized conductance. This regime is dominated by electron-electron interactions, which are known to reduce the quantized conductance [40]. The evolution of 1D subbands may be further visualized in the grayscale plot in Fig. 6(b), which shows the transconductance of the results presented in Fig. 6(a). The conductance data for V_{tg} from 0 to -1.80 V exhibit regular integer plateaus, however, they are not included here. It may be noted that on moving to more negative top gate voltages, before the first plateau disappears, there is an anticrossing of the first $(4e^2/h)$ and second $(6e^2/h)$ excited states, due to the weakening of 4e²/h at V_{tg} ~-2.6 V. However, this is a short-lived state as V_{tg} is gradually made more negative, around V_{tg} =-2.9 V, the ground $(2e^2/h)$ and first excited states anticross, resulting in the disappearance of $2e^2/h$, and the new ground state is now $4e^2/h$, shown with an arrow in Fig. 6(b). To be noted that there is a tendency for the disappearance of the third plateau $(6e^2/h)$, on making the top gate more negative; however, this was hard to measure as the regime was in close proximity to the 2D regime. The anticrossing of the ground and first excited states indicates the possible reorganization of 1D electrons into a zigzag to form a 1D Wigner lattice. Our results are in agreement with previous findings [4,5,32].

The results shown in Figs. 5 and 6 come from two different samples, although both were fabricated from the same GaAs/AlGaAs wafer. One displays interaction effects, while the other does not. This difference may result from the complex interplay between carrier density and the confinement potential, which is shaped by the split gates and the top gate. Moreover, to observe the anticrossing, it is crucial that not only a low-density 1D regime is present, but also that the interaction energy exceeds the confinement energy for a 1D Wigner lattice to form.

We notice signatures of electron-electron interaction effects near the 1D-2D transition in Sample B, where the interaction effects dominate the confinement and kinetic energies. To determine if the 1D regime has conditions for the formation of the 1D Wigner lattice, we need to estimate the 1D density of electrons, n_{1D} . The 2D density, n_{2D} , along the 1D channel may be estimated using the channel pinch-off voltage, V_D using the relation

$$n_{2D} = \varepsilon \varepsilon_0 V_p / 2\pi eW, \tag{1}$$

where ε =12.5 is the dielectric constant of GaAs, ε_0 is the permittivity of free space, and e is the electron charge [16,41,42]. As the Wigner lattice forms in the ground state, the effective width of the channel can be approximated to $\lambda_{2D}/2$, where, $\lambda_{2D} = (2\pi/n_{2D})^{1/2}$ is the Fermi wavelength of the 2DEG, therefore.

$$n_{ID} = n_{2D} \lambda_{2D}/2 \tag{2}$$

may be estimated [18]. For the anticrossing in Fig. 6, the effective pinch-off voltage, V_p^* due to both split and top gates is \sim - 5.0 V. Using (1) and (2), we get $n_{2D} \sim 5.6 \times 10^{10}$ cm⁻², and $n_{1D} \sim 2.75 \times 10^5$ cm⁻¹. As $n_{1D} a_B < 1$, where $a_B = 10$ nm is the effective Bohr radius of GaAs, a 1D Wigner crystal may have appeared in the system.

In conclusion, we created 1D channels using high-quality 2DEGs and studied electron transport within them. By carefully adjusting the confinement and density of 1D electrons, we observed potential signs of a 1D Wigner lattice. Our findings suggest that 1D quantum systems hold great potential for exploring different phases expected to form within the Wigner regime.

V. References

- [1] T. J. Thornton, M. Pepper, H. Ahmed, D. Andrews, and G. J. Davies, "One-dimensional conduction in the 2D eelctron gas of a GaAs-AlGaAs Heterojunction," *Phys. Rev. Lett.*, vol. 56, no. 11, pp. 1198-1201, 1986.
- [2] K. F. Berggren, T. J. Thornton, D. J. Newson and M. Pepper, "Magnetic Depopulation of 1D Subbands in a Narrow 2D Electron Gas in a GaAs:AlGaAs Heterojunction," *Phys. Rev. Lett.*, vol. 57, p. 1769, 1986.
- [3] K-F. Berggren and M. Pepper, "Electrons in one dimension," *Philos. Trans. R. Soc. London, Ser. A*, vol. 368, no. 1914, pp. 1141-1162, 2010.
- [4] S. Kumar, K. J. Thomas, L. W. Smith, M. Pepper, G. L. Creeth, I. Farrer, D. Ritchie, G. Jones, and J. Griffiths, "Many-body effects in a quasi-one-dimensional electron gas," *Phys. Rev. B*, vol. 90, no. 20, p. 201304, 2014.
- [5] S. Kumar and M. Pepper, "Interactions and non-magnetic fractional quantization in one-dimension," *Appl. Phys. Lett.*, vol. 119, no. 11, p. 110502, 2021.
- [6] D. A. Wharam, T. J. Thornton, R. Newbury, M. Pepper, H. Ahmed, J. E. F. Frost, D. G. Hasko, D. C. Peacock, D. A. Ritchie, and G. A. C. Jones, "One-dimensional transport and the quantisation of the ballistic resistance," *J. Phys. C*, vol. 21, no. 8, pp. L209-L214, 1998.
- [7] K. J. Thomas, J. T. Nicholls, M. Y. Simmons, M. Pepper, D. R. Mace, and D. A. Ritchie, "Possible spin polarization in a one-dimensional electron gas," *Phys. Rev. Lett.*, vol. 77, no. 1, pp. 135-138, 1996.
- [8] S. Kumar, M. Pepper, D. A. Ritchie, I. Farrer, and H. Montagu, "Formation of a non-magnetic, odd-denominator fractional quantized conductance in a quasi-one-dimensional electron system," *Appl. Phys. Lett.*, vol. 115, no. 12, p. 123104, 2019.
- [9] S. Kumar, M. Pepper, S. N. Holmes, H. Montagu, Y. Gul, D. A. Ritchie, and I. Farrer, "Zero-Magnetic Field Fractional Quantum States," *Phys. Rev. Lett.*, vol. 122, no. 8, p. 086803, 2019; S Kumar, et al. "Effect of low transverse magnetic field on the confinement strength in a quasi-1D wire." *AIP Conf. Proc.*, Vol. 1566. No. 1, p.245-246, 2013

- [10] B. J. van Wees, H. van Houten, C. W. J. Beenakker, J. G. Williamson, L. P. Kouwenhoven, D. van der Marel, and C. T. Foxon, "Quantized conductance of point contacts in a twodimensional electron gas," *Phys. Rev. Lett.*, vol. 60, no. 9, pp. 848-850, 1988.
- [11] M. Büttiker, "Quantized transmission of a saddle-point constriction," *Phys. Rev. B*, vol. 41, no. 7906, pp. 7906-7909, 1990.
- [12] L. W. Smith, A. R. Hamilton, K. J. Thomas, M. Pepper, I. Farrer, J. P. Griffiths, G. A. C. Jones, and D. A. Ritchie, "Compressibility Measurements of Quasi-One-Dimensional Quantum Wires," *Phys. Rev. Lett.*, vol. 107, no. 12, p. 126801, 2011.
- [13] F. Sfigakis, C. J. B. Ford, M. Pepper, M. Kataoka, D. A. Ritchie, and M. Y. Simmons, "Kondo effect from a tunable bound state within a quantum wire," *Phys. Rev. Lett.*, vol. 100, no. 2, p. 026807, 2008.
- [14] K. J. Thomas, J. T. Nicholls, M. Pepper, W. R. Tribe, M. Y. Simmons, and D. A. Ritchie, "Spin properties of low-density one-dimensional wires," *Phys. Rev. B*, vol. 61, no. 20, pp. R13365 R13368, 2000.
- [15] N. Bhandari, P. P. Das, M. Cahay, R. S. Newrock, and S. T. Herbert, "Observation of a 0.5 conductance plateau in asymmetrically biased GaAs quantum point contact," *Appl. Phys. Lett.*, vol. 101, no. 10, p. 102401, 2012.
- [16] H. Montagu, I. Farrer, D. Ritchie, and S. Kumar, "Spin polarised quantum conductance in 1D channels," *Applied Physics Express*, vol. 18, no. 1, p. 015002, 2025.
- [17] L. Calmels and A. Gold, "Spin-polarized electron gas in quantum wires: Anisotropic confinement model," *Solid State Commun.*, vol. 106, no. 3, pp. 139-143, 1998.
- [18] V. Kumar, Y. Duo, P. See, J. P. Griffiths, D. A. Ritchie, I. Farrer, and S. Kumar, "Correlation effects mediated by disorders in one-dimensional channels," *Phys. Rev. B*, vol. 112, no. 3, p. 035404, 2025.
- [19] K. J. Thomas, J. T. Nicholls, N. J. Appleyard, M. Y. Simmons, M. Pepper, D. R. Mace, W. R. Tribe, and D. A. Ritchie, "Interaction effects in a one-dimensional constriction," *Phys. Rev. B*, vol. 58, no. 8, pp. 4846 4852, 1998.
- [20] C-K. Wang and K-F. Berggren, "Spin splitting of subbands in quasi-one-dimensional electron quantum channels," *Phys. Rev. B*, vol. 54, no. 20, pp. 14257-14260, 1996.
- [21] K-F. Berggren and I. I. Yakimenko, "Effects of exchange and electron correlation on conductance and nanomagnetism in ballistic semiconductor quantum point contacts," *Phys. Rev. B*, vol. 66, no. 8, p. 085323, 2002.
- [22] A. E. Feiguin and G. A. Fiete, "Spin-incoherent behavior in the ground state of strongly correlated systems," *Phys. Rev. Lett.*, vol. 106, no. 14, p. 146401, 2011.
- [23] S. Kumar, M. Pepper, H. Montagu, D. Ritchie, I. Farrer, J. Griffiths, and G. Jones, "Engineering electron wavefunctions in asymmetrically confined quasi one-dimensional structures," *Appl. Phys. Lett.*, vol. 118, no. 12, p. 124002, 2021.
- [24] W. K. Hew, K. J. Thomas, M. Pepper, I. Farrer, D. Anderson, G. A. C. Jones, and D. A. Ritchie, "Spin-incoherent transport in quantum wires," *Phys. Rev. Lett.*, vol. 101, no. 3, p. 036801, 2008.
- [25] L. W. Smith, H. B. Chen, C. W. Chang, C. W. Wu, S. T. Lo, S. H. Chao, et al, "Electrically Controllable Kondo Correlation in Spin-Orbit-Coupled Quantum Point Contacts," *Phys. Rev. Lett.*, vol. 128, p. 027701, 2022.
- [26] K. A. Matveev, "Conductance of a quantum wire at low electron density," *Phys. Rev. B*, vol. 70, no. 24, p. 245319, 2004.
- [27] K. A. Matveev, "Conductance of a quantum wire in the Wigner-crystal regime," *Phys. Rev. Lett*, vol. 92, no. 10, p. 106801, 2004.
- [28] J. S. Meyer and K. A. Matveev, "Wigner crystal physics in quantum wires," *J. Phys.: Condens. Matter*, vol. 21, no. 2, p. 023203, 2009; A. V. Chaplik, "Instability of quasi-one-dimensional electron chain and the "string-zigzag" structural transition." *JETP Lett.* vol. 31(5)

- pp. 275-27, 1980; E. Wigner, "On the interaction of electrons in metals." *Phys. Rev.* vol. 46, p. 1002, 1934.
- [29] B. Antonio, A. Bayat, S. Kumar, M. Pepper, and S. Bose, "Self-assembled wigner crystals as mediators of spin currents and quantum information," *Phys. Rev. Lett.*, vol. 115, no. 21, p. 216804, 2015.
- [30] I. Shapir, A. Hamo, S. Pecker, C. P. Moca, Ö. Legeza, G. Zarand and S. Ilani, "Imaging the electronic Wigner crystal in one dimension," *Science*, vol. 364, no. 644, pp. 870-875, 2019.
- [31] C. Mehta, C. J. Umrigar, J. S. Meyer, and H. U. Baranger, "Zigzag phase transition in quantum wires," *Phys. Rev. Lett.*, vol. 110, no. 24, p. 246802, 2013.
- [32] W. K. Hew, K. J. Thomas, M. Pepper, I. Farrer, D. Anderson, G. A. C. Jones, and D. A. Ritchie, "Incipient formation of an electron lattice in a weakly confined quantum wire," *Phys. Rev. Lett.*, vol. 102, no. 5, p. 056804, 2009.
- [33] S-C. Ho, H-J. Chang, C-H. Chang, S-T. Lo, G. Creeth, S. Kumar, I. Farrer, D. Ritchie, J. Griffiths, and G. Jones, "Imaging the Zigzag Wigner Crystal in Confinement-Tunable Quantum Wires," *Phys. Rev. Lett.*, vol. 121, no. 10, p. 106801, 2018.
- [34] R. A. Bruce and G. R. Piercy. "An improved Au/ Ge/Ni ohmic contact to n-type GaAs." *Solid-State Electronics* 30.7 (1987): 729-737
- [35] E. J. Koop, et al. "On the annealing mechanism of AuGe/Ni/Au ohmic contacts to a two-dimensional electron gas in GaAs/AlxGal-xAs heterostructures." Semiconductor science and technology 28.2 (2013): 025006.
- [36] A. G. Baca and C. I. Ashby, Fabrication of GaAs devices, IET, 2005...
- [37] G. S. Saravanan, et al. "Ohmic contacts to pseudomorphic HEMTs with low contact resistance due to enhanced Ge penetration through AlGaAs layers." *Semiconductor science and technology* 23.2 (2008): 025019.
- [38] S. Tahamtan, et al. "Investigation on the effect of annealing process parameters on AuGeNi ohmic contact to n-GaAs using microstructural characteristics." *Microelectronics Reliability* 51.8 (2011): 1330-1336.
- [39] W.T. Masselink, et al. "The dependence of 77 K electron velocity-field characteristics on low-field mobility in AlGaAs-GaAs modulation-doped structures." *IEEE transactions on electron devices* 33.5 (1986): 639-645; R. P. Taylor, P. T. Coleridge, M. Davies, Y. Feng, J. P. McCaffrey, and P. A. Marshall, "Physical and electrical investigation of ohmic contacts to AlGaAs/GaAs heterostructures," *J. Appl. Phys.*, vol. 76, no. 12, p. 7966–7972, 1904
- [40] A. Yacoby, H. L. Stormer, N. S. Wingreen, L. N. Pfeiffer, K. W. Baldwin, and K. W. West, "Nonuniversal conductance quantization in quantum wires," *Phys. Rev. Lett.*, vol. 77, no. 22, pp. 4612-4615, 1996.
- [41] Y. V. Nazarov and Y. M. Blanter, Quantum Transport, Cambridge: Cambridge University Press, 2009.
- [42] L. I. Glazman and I. A. Larkin, "Lateral position control of an electron channel in a split-gate device," *Semicond. Sci. Technol.*, vol. 6, no. 1, pp. 32 35, 1991.